# Beach Erosion and Sand Transport at Hunting Island, South Carolina, USA

## James P. May† and Frank W. Stapor, Jr.‡

†Department of Chemistry
  and Geology
The Citadel
Charleston, SC 29409, U.S.A.

‡Department of Earth
  Sciences
Tennessee Technological
  University
Cookeville, TN 38505, U.S.A.

ABSTRACT

MAY, J.P. and STAPOR, F.W., 1996. Beach Erosion and Sand Transport at Hunting Island, South Carolina, USA. *Journal of Coastal Research*, 12(3), 714–725. Fort Lauderdale (Florida). ISSN 0749-0208.

Hunting Island has experienced major shoreline erosion over the past 140 years. The beach has lost sand at the rate of approximately 130,000 m³/year. Over the period 1920–1971, the shoreline retreated 5–7 m/year. Beach renourishment has essentially stabilized the shoreline since 1968. Extensive shoals of the St. Helena Sound ebb tidal delta shield the island from northeast waves. Farther south, the Hunting Island Platform impedes waves approaching from east through southeast. Sediments occurring on the platform and beach are dominantly medium-to-fine sand. Computer simulation of longshore sand transport using the WAVENRG model predicts a gross longshore drift of about 100,000 m³/year and a net longshore drift to the north along Hunting Island of about 12,000 m³/year. Flood tidal currents dominate along the Hunting Island nearshore. These currents flow westward toward the coast, then northward into St. Helena Sound. It is concluded that sand is being suspended in the nearshore zone by waves, causing beach erosion, and transported northward into St. Helena Sound by longshore and flood tidal currents. Most of this sand is then swept seaward through ebb-dominated tidal channels to be deposited on the outer Hunting Island Platform. Shoaling waves transport the sand landward to a depocenter along the inner margin of the outer platform. Sand that is able to bypass this depocenter is delivered to the funnel-shaped inner platform. As the inner platform is largely flood-dominated, the sand entrained by waves is transported by flood tidal currents northward to St. Helena Sound. The Hunting Island beach is effectively isolated from any offshore source of replenishing sand. Similar sand transport systems can be expected to exist in regions characterized by similar morphodynamic attributes.

ADDITIONAL INDEX WORDS: *Longshore sand transport, shoreline erosion, tidal channels, coastal morphodynamics.*

## INTRODUCTION

Hunting Island is located on the southern South Carolina coast (Fig. 1). For more than 100 years, the beach at Hunting Island eroded at a net rate of about 130,000 m³/year (STAPOR and MAY, 1981) resulting in a shoreline retreat rate of about 5–7 m/year. The U. S. Army Corps of Engineers began an erosion control project in 1968 that consisted of a 3050 m feeder beach and a 250 m terminal groin located at the island's northern tip. Five separate nourishment operations totaling 4.9 million cubic meters of sand have been completed since the project was authorized. The most recent occurred in 1991 (CSE, 1990; CSE, 1991). The present study was undertaken in a effort to better understand the cause of erosion and to provide information that could assist in the formulation of a successful management plan for the state park located on the island.

## STUDY AREA

Hunting Island is a Holocene barrier typical of the mesotidal, northeast-southwest oriented South Carolina coast (Fig. 2). The island consists of several beach-ridge sets, the

oldest of which is at least 1500 years old (STAPOR and MATHEWS, 1983). Individual beach ridges are 2–3 m in elevation and have a spacing of 50–75 m. These ridges are composed of fine-grained quartz sand with minor amounts of heavy minerals.

St. Helena Sound lies immediately northeast of Hunting Island (Fig. 1). It is a wide estuary characterized by numerous shoals and tidal channels. The major tidal channels in St. Helena Sound are essentially perpendicular to the coastline orientation, but curve to the south near their mouths.

The major portion of the St. Helena Sound ebb tidal delta, herein termed the "Hunting Island Platform", is located seaward of Hunting Island or to the south of St. Helena Sound. The Hunting Island Platform can be divided into two parts: (1) an outer platform that is located in the northern and eastern part of the study area and is characterized by deep tidal channels and marginal and distal shoals; and (2) the funnel-shaped, inner platform that is located between the island and the outer platform. The bathymetry of the platform is such that depths of 1 to 2 m (mean low water) are encountered up to 10 kilometers offshore. There are extensive areas where depths are less than 3 m. The 6 m isobath lies as much as 12 kilometers off Hunting Island and forms the outer boundary of the platform. By comparison, the 6 m isobath is only
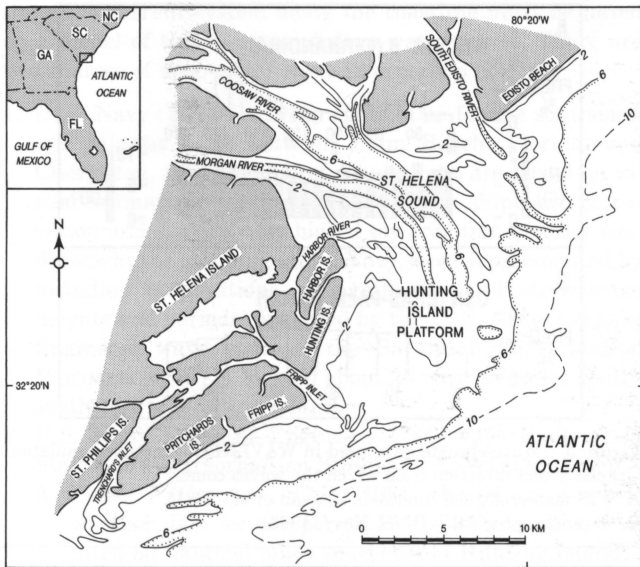
Figure 1. Generalized location map of the Hunting Island area, Beaufort County, South Carolina. The 6-meter isobath delineates the Hunting Island Platform. The outer platform is located in the north and east portion of the study area and is characterized by shoals and channels. The inner platform is the funnel-shaped region between the outer platform and Hunting Island.
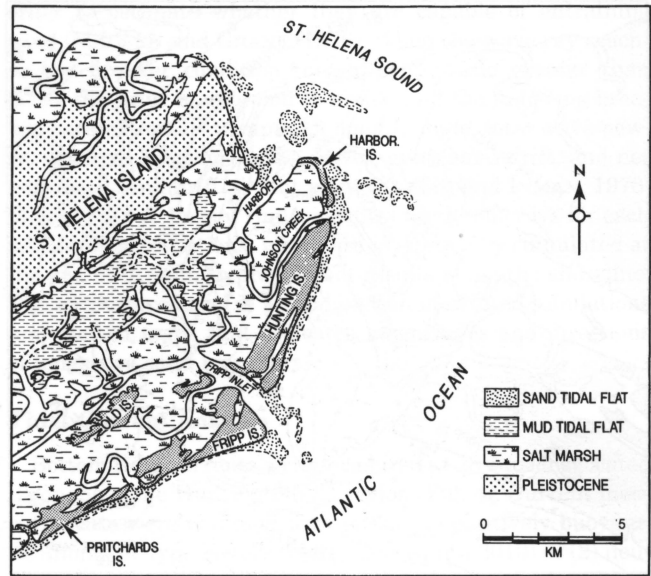


Figure 2. Map of geomorphology/geology of the Hunting Island region.

2 kilometers off Edisto Island (to the north across St. Helena Sound) and 4 kilometers off Pritchards Island (the second island to the south).

Platform sediments consist of relatively clean sand to a depth of about −7 m (mlw) with minor occurrences of mud flasers (CSE, 1991). Based on the analysis of thirty-five vibracores averaging about 3.5 m in length from various locations on the platform in water depths of 3 to 4 m (mean low water), CSE reported no indication of pre-Holocene materials. The platform was apparently constructed during late Holocene time and has consisted of easily erodable sand for several thousand years.

Mean tidal range at Hunting Island is 6.2 feet. Spring tidal range is 7.2 feet and neap tidal range is 5.2 feet. The regional orientation of the coastline is about N45E, though the Hunting Island shoreline is oriented at N21E. Therefore, only waves from the east-southeast quadrant of the compass have a significant effect on the coast. Deep water wave height averages 1 meter and period averages 6.5 seconds.

The broad, shallow platform off Hunting Island should act as a buffer that shields the beach from the large waves from the Atlantic Ocean, especially storm waves. Waves encounter shallow depths nearly 10 km offshore and much of their energy is expended in the process of transiting the shallow depths of the platform resulting in waves arriving at the beach that are smaller than they would be in the absence of the platform. Hunting Island's location behind such a platform should ensure that it would experience less beach erosion in comparison with more exposed barrier islands to the north and south. To the contrary, Hunting Island has expe-

rienced coastal erosion comparable to and even exceeding that of the more exposed South Carolina barriers (STEPHEN, BROWN, FITZGERALD, HUBBARD, and HAYES, 1975; HUBBARD, BARWIS, LESESNE, STEPHEN, and HAYES, 1977).

## METHODS

### Bathymetric Analysis

The historic changes in the position of the shoreline at Hunting Island (Fig. 3) over the interval 1859–1982 were obtained from ANDERS et al. (1990). Shoreline movement rates were computed by dividing the distance moved by the time interval between surveys.
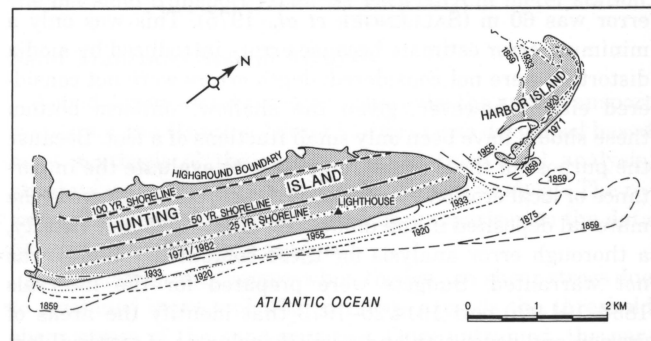


Figure 3. Hunting Island shorelines from 1859 to 1971/82 mapped by the National Ocean Survey and its predecessors. The 25-, 50-, and 100-year shorelines are extrapolated from the 1920–1971 average retreat rate of 5–7 m/year and indicate the future positions of the shoreline in the absence of preventive measures. Artificial beach renourishment has essentially eliminated further shoreline recession since 1971.
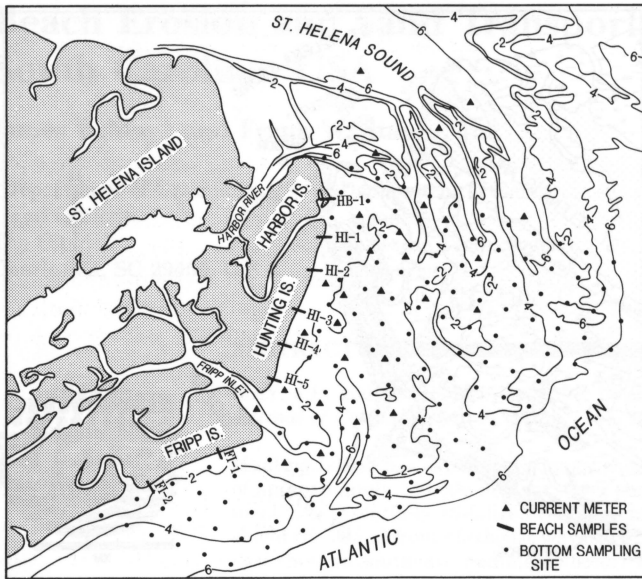
Figure 4.  Location map for Hunting Island beach and platform sand samples. Each beach transect was sampled at eight to twelve sites with 5 replicate samples taken at each site. Platform samples were taken on a one kilometer-square grid. Bottom tidal currents were measured at the sites marked by the solid triangles.
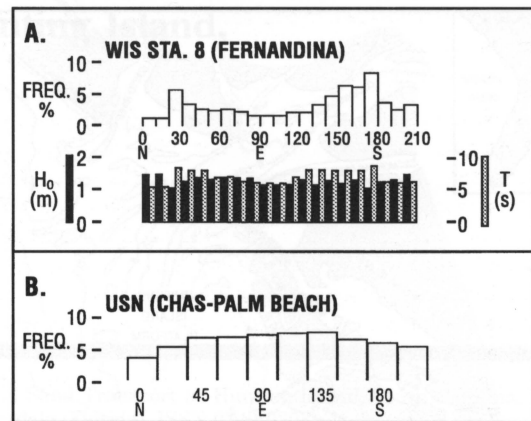


Figure 5.  Wave-climate data used in WAVENRG computer simulation. Graphs depict direction from which the waves come:
A. WIS meteorological hindcasts (Corson et al., 1981),
B. Oceanographic Atlas (U. S. Navy, 1963).

Historic sand budgets were inferred from an analysis of sequential changes in bathymetry (PIERCE, 1969; STAPOR, 1971). This technique involved subtracting a depth matrix from a previous one to determine whether erosion (depth increase) or deposition (depth decrease) had taken place. The resulting difference matrix was contoured and the areas of erosion and deposition were determined by planimetry. The volumes of material eroded and deposited were computed by multiplying the contour-line area by the contour interval. An error estimate was made by adding and subtracting the joint horizontal error in sounding location to the radius of the circle equal to the area enclosed by the contour line. In the case of these 1:20000 scale surveys the joint horizontal location error was 60 m (SALLENGER et al., 1975). This was only a minimum error estimate because errors introduced by media distortion were not considered; depth errors were not considered either, however, given the shallow, uniform bottom these should have been only small fractions of a foot. Because the purpose of these measurements is to evaluate the importance of local erosion versus external sources to generate the material deposited in the immediate Hunting Island vicinity, a thorough error analysis for these computed volumes was not warranted. Budgets were prepared for the intervals 1856–1914/20 and 1914/20–1973 that identify the areas of erosion and deposition and quantify volumes of material lost or gained.

## Sand Analysis

Sands were sampled from the Hunting Island beach and offshore region and were analyzed in an effort to relate the distribution of sands to erosional and depositional patterns as revealed by bathymetric differencing. From the beaches of Harbor, Hunting and Fripp Islands (Fig. 4), five replicate sand samples were collected from each of 80 sites located along 8 beach transects. From the Hunting Island Platform, 143 bottom samples were collected with a Dietz/Lafond grab sampler on a one kilometer-square grid from the shoreline out to the 6 m (20 ft) isobath.

The sand samples were split and analyzed for calcium carbonate, heavy minerals, sand/silt/clay percentages, and the distribution of settling speeds of the sand fraction. Calcium carbonate content was determined by HCl digestion. Heavy minerals were separated by magnetic and heavy liquid methods. Sand/silt/clay percentages were determined by wet sieving and pipette analysis.

The sand fraction was subjected to settling tube analysis. The distribution of sand settling speeds as determined by settling tube analysis is shown in CHI ($\chi$) units (MAY, 1981) defined as:

$$\chi = -\log_2(s/s_0)$$

where s is measured settling speed and $s_0$ is the standard settling speed of 1 m/s at 20 degrees C.

Though there is some inaccuracy involved, particle diameter ($\phi$ and mm) can be approximated from $\chi$ units by the relationship:

$$\text{Diam}_\phi = -3.79 + 3.68 \ln \chi$$
$$\text{Diam}_{mm} = e^{-\phi}$$

Note that smaller $\chi$ values correspond to faster (coarser) particles. Moment statistics were computed based on the distribution of settling speeds.

## Wave Current Analysis

Long-term observations of wave parameters (statistical distributions of height, period, and direction) for the Hunting

Island coastal region do not exist; therefore, a description of the wave current system along the coastline must be based on a model of the shoaling of deep-water waves. There are two sources of deep-water wave information (Fig. 5):

1. U. S. Navy (1963) Oceanographic Atlas for the southeastern Atlantic coast between Palm Beach, Florida, and Charleston, South Carolina. These data are based on visual estimates of wave parameters from shipboard observation and are probably biased towards fair weather conditions in the shipping lanes. They were supplemented by including observations of significant- and storm-wave heights and periods measured by the U. S. Army Corps of Engineers wave gage at the Savannah Light station (THOMPSON, 1977), located about 25 nautical miles south-southwest of Hunting Island.
2. U.S. Army Corps of Engineers Waterways Experiment Station Wave Information Studies (WESWIS) hindcasts:
   A. Phase I (CORSON et al., 1981)—based on synoptic weather data for the period 1956–75 for Station 8 located 80 nautical miles southeast of Hunting Island.
   B. Phase II (CORSON et al., 1982)—based on synoptic weather data for the period 1956–75 and on Phase I output for Station 54 (water depth 80 feet) located 35 nautical miles southeast of Hunting Island.
   C. Phase III (JENSEN, 1983)—based on output from Phase II studies computed for Station 121 (water depth 10). This data was determined to be unusable because (1) the Hunting Island Station (No. 121) was located in the intertidal zone and not in 10 m water depth and (2) was based on an unrealistic assumption of straight and parallel bathymetric contours. The computer model described below is believed to provide a superior estimate of shoreline wave conditions.

The WAVENRG model is based on the tracking of the refracted path of individual wave orthogonals (rays) from deep water to the beach and has been shown to adequately describe wave shoaling characteristics and longshore drift vectors (MAY and TANNER, 1973; MAY, 1974; GREENWOOD and McGILLIVRAY, 1978; LOWRY and CARTER, 1982, CARTER, JENNINGS, and ORFORD, 1990; STONE, STAPOR, MAY, and MORGAN, 1992). Input for WAVENRG includes a bathymetric matrix; tidal-stage elevations; and a frequency distribution for deep-water wave heights, periods, and approach directions. A bathymetry grid ( 1 cm. nodal spacing) is constructed on a regional scale (1:80,000) for offshore waters and local scale (1:40,000) for nearshore waters in order to permit computations at finer detail near the shoreline. Starting with deep-water conditions, WAVENRG tracks a wave ray shoreward. Refraction of the ray due to changing water depth is constantly computed at small increments along the ray path. At each incremental position, wave height and energy density are recomputed, taking into account energy dissipation due to bottom friction and concentration changes due to convergence and divergence of adjacent rays. Also computed and stored are the maximum wave orbital velocities at the bottom based on linear theory (AIRY, 1856). Linear theory has been determined to adequately represent maximum wave orbital velocities near the bottom in shallow water (MAY, 1976).

These velocities can be converted to bottom shear stress in order to estimate whether they are capable of entraining sand (MADSEN and GRANT, 1976). When the wave ray reaches the breaker condition (height/depth ratio greater than 0.78), the wave is assumed to break, and the following breaker parameters are computed: height, angle, total wave-power, effective longshore wave-power, gross sand drift, and net longshore sand drift at that point (KOMAR and INMAN, 1970; MAY, 1973). A normal run consists of numerous rays for each set of initial conditions, which are algebraically cumulated at the end of the run to provide net results along the shoreline. The output produced is a combination of printed tabulations and plotted maps that indicates magnitudes and directions of longshore sand transport.

## Tidal Current Analysis

Bottom tidal currents were measured at 28 stations located throughout the Hunting Island region (Fig. 4). Current measurements were obtained with either (1) positively buoyant, inclinometer-type meters (General Oceanics 2010) or (2) neutrally buoyant, ducted impeller-type meters (Endeco 174). The meters were positioned one meter above the bottom and were deployed for periods of about five days during which current vector information was recorded at a rate of 16 measurements per hour.

As all deployments were not synoptic, it was necessary to compare the results of different deployments to determine whether sampling of different parts of the monthly lunar cycle caused significant errors. That is, some data sets were influenced more by spring tides and some by neap tides. Analysis of the data indicated that these errors were less than 10% for the range of currents measured in the study area.

Tidal current data were synthesized by plotting current vectors versus time for each station in order to identify obvious errors. The data were then smoothed and filtered to remove noise. Partial coverage of starting and ending tidal cycles were identified and eliminated in order to produce a record of an integer number of tidal cycles. These data were used by the sand transport model described below to estimate the net sand transport vector for each current meter station.

## Sand Transport System Analysis

A model that would reasonably describe the sand transport system for the Hunting Island Platform was developed based on a synthesis of the results derived from sand analysis, shoaling wave simulation, and tidal current analysis. The results of the model were evaluated by comparison to the data derived by bathymetric analysis.

Sand entrainment occurs when the bottom shear stress due to combined wave and tidal currents exceeds the threshold shear stress of the sand particles. Once entrained, the particles are subject to net transport by unidirectional tidal currents and by asymmetrical wave currents. Numerous studies have addressed the determination of the entrainment threshold stress and mass transport equations (SHIELDS, 1936; BAGNOLD, 1946; MANOHAR, 1955; SUNDBORG, 1956; BAGNOLD, 1963; STERNBERG, 1972; KOMAR and MILLER, 1973;

MADSEN and GRANT, 1975; KOMAR and MILLER, 1975; SWART, 1976; MILLER and KOMAR, 1977; GRANT and MADSEN, 1979; HAMMOND and COLLINS, 1979; LARSEN *et al.*, 1981). These studies conclude generally that some version of the Shields criterion adequately describes the entrainment threshold.

We used the relationship developed by KOMAR and MILLER (1973, 1975) to establish the threshold criterion for Hunting Island platform sediments:

$$\Theta_t = \frac{\rho u_m^2}{(\rho_s - \rho)gD} = 0.21(d_0/D)^{0.5}$$

where $d_0$ = orbital diameter (all in cgs units), and the empirical constant of 0.21 for grain diameters less then 0.05 cm only. Bottom fluid orbital velocity and diameter are given by:

$$u_m = \frac{\pi H}{T \sinh(2\pi H/L)}$$

and

$$d_0 = Tu_m/\pi$$

where H is wave height, T is wave period, and L is wavelength. They provided a computer program that determines threshold values of $u_m$ for specified sediment diameters.

PATTIARATCHI and COLLINS (1985) tested 10 different sand transport equations and concluded that those developed by MADSEN and GRANT (1976) and STERNBERG (1972), as modified for the presence of waves by SWART (1976), best described their sand transport data obtained by tracer study in the northern Bristol Channel. We used the STERNBERG/SWART formulas for computing the mass transport rate. The Sternberg equation for mass transport rate due to a unidirectional current is (STERNBERG, 1972):

$$j = \frac{K\rho U*_c^3 \rho_s}{g(\rho_s - \rho)} \quad (gm/cm/sec)$$

where:

K is a function of the excess shear stress $((\tau_0 - \tau_t)/\tau_t)$ and the particle diameter (D). $\tau_0$ is the bed shear stress and $\tau_t$ is the threshold shear stress.
U*$_c$ is the friction velocity due to unidirectional current.
$\rho$ is water density.
$\rho_s$ is sediment density.
g is acceleration of gravity.

The SWART modification (SWART, 1976) involves substituting U*$_{wc}$ for U*$_c$ to account for the presence of currents due to waves:

$$U*_{wc} = U*_c(1 + 0.5(\xi U_m/U)^2)^{0.5}$$

where:

$\xi$ is a function of the Chezy coefficient (ROUSE, 1938) and JONSSON's friction factor (JONSSON, 1966).
U is the depth-averaged current velocity.
$U_m$ is the maximum wave orbital velocity.

Using the wave refraction program WAVENRG, a distribution of bottom orbital velocities (based on linear theory) was computed for each set of typical wave conditions, weighted for frequency of occurrence. Based on the equations above, the bed shear stress was computed for each current meter site. If, at a given location, the threshold for sediment entrainment was exceeded, a sediment transport value was computed as described above. These values were integrated and averaged over an integer number of tidal cycles measured to provide an estimate of the sand transport vector at that location.

Tidal currents were characterized by determining separately the mean vectors for ebb and flood currents. The vector with the greater magnitude indicates directional dominance. The magnitude was computed by adding the ebb and flood magnitudes algebraically. This method was used because ebb and flood current vectors were not always co-linear. A net resultant would have been misleading unless the ebb and flood direction modes were exactly 180 degrees opposed, a condition that was not frequently encountered. For example, alternating tidal currents directed at azimuth 010 and 170 degrees at a station located in a curving tidal channel that runs generally north-south produce a net resultant that indicates a current directed to the east, across the axis of the channel. Comparison of the magnitudes of the bidirectional resultant vectors can indicate whether the 010 or the 170 degree current dominates, a more significant piece of information. The sand transport magnitude was considered to be traveling in the direction of the dominant tidal flow.

## RESULTS

### Bathymetric Analysis

Historic shoreline erosion at Hunting Island (Fig. 3) as documented by detailed topographic and photogrammetric surveys (ANDERS, *et al.*, 1990) encompasses two distinct periods:

(1) Between 1859 and 1920, erosion removed 2 km of the spit-like northern end of the island that extended northeastward into St. Helena Sound. At the southern end of the island, the shoreline retreated about 300 m. In the remaining central portion of the island, the shoreline advanced about 120 m seaward.

(2) From 1920 to 1982 the shoreline retreated uniformly along the entire island a distance of 250–350 m except at the extreme southern tip of the island where the shoreline prograded seaward about 250 m between 1955 and 1968. The average mean-high-water shoreline retreat between 1920 and 1982 was 5–7 m/year.

If these rates were extrapolated into the future, in the absence of defensive measures, shoreline retreat would have toppled the Hunting Island lighthouse by 1993 and should destroy the entire barrier island (ignoring washover) by 2070. Because of defensive measures taken, the lighthouse is still standing. Beginning in 1968, five separate beach nourishment projects by the U. S. Army Corps of Engineers were completed in an attempt to stabilize the shoreline position. Between February 1968 and April 1991, these projects had placed a total of 4.9 million cubic meters of fill on the beach.

Map differencing indicates that during the 1856–1914/20 (64 years) interval Hunting Island and its immediate nearshore region (areas 1–9) experienced total erosion of 16.14
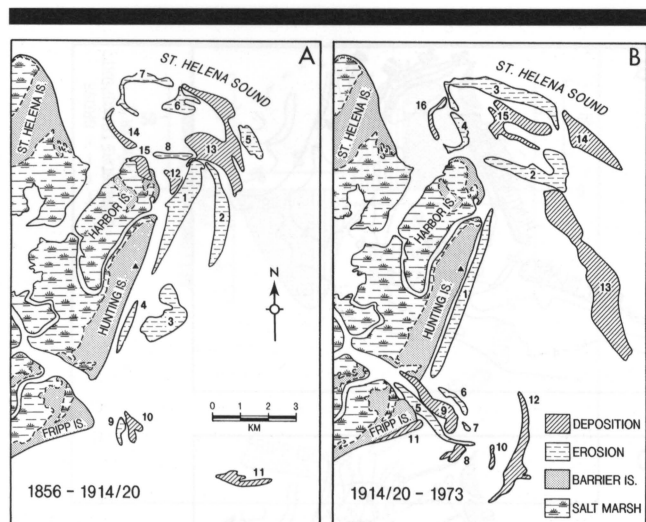
Figure 6. Areas of net erosion and deposition identified in the Hunting Island area by the map differencing technique for:
A. 1856–1914/20, and B. 1914/20–1973; The two patterns of Hunting Island erosion are clearly observable: 1) the initial retreat of the spit-like promontory over the interval 1856–1920 and 2) the relatively uniform retreat of the entire island since 1920. The volumes of each area are presented in Tables 1 and 2.

Table 1B. *Erosion and deposition volumes for the interval 1914/20–1973. These areas are located in Figure 6B. Volumes are X 10³ m³. The Hunting Island Platform is that part of the St. Helena Sound ebb tidal delta adjacent to the southern part of the sound and Hunting Island.*

| Location | Erosion | | Deposition | |
|---|---|---|---|---|
| | Area | Volume | Area | Volume |
| Hunting Island Region | 1 | 6,950 ± 1,230 | | |
| St. Helena Sound (southern part) | 2 | 4,330 ± 950 | 14 | 4,980 ± 1,130 |
| | 3 | 6,090 ± 137 | 15 | 1,720 ± 390 |
| | 4 | 1,050 ± 430 | 16 | 170 ± 140 |
| Fripp Inlet | 5 | 4,020 ± 1,050 | 8 | 240 ± 100 |
| | 6 | 380 ± 250 | 9 | 4,090 ± 1,050 |
| | 7 | 120 ± 120 | 10 | 200 ± 1,500 |
| | | | 11 | 490 ± 220 |
| Hunting Island Platform | | | 12 | 2,230 ± 450 |
| | | | 13 | 10,130 ± 1,320 |

million m³ or an average net erosion rate of 252,000 m³/year (Fig. 6A and Table 1A). About 60% of this loss occurred as a result of the removal of the northern third of the island (area 1) and an associated shoal (area 2). The remaining areas of erosion comprised various shoals in St. Helena Sound, off central Hunting Island, and near Fripp Island inlet. Loss from the shoreline of Hunting Island (area 4) was minor (about 2% of the total).

Total deposition in the region over the same time interval amounted to 13.45 million m³ or an average net deposition rate of 210,000 m³/year. About 88% of the deposition occurred in St. Helena Sound (areas 12, 13, 14, and 15). All but area 15, the northern tip of Harbor Island, are subtidal shoals. Area 13 contains about 80% of the material deposited in the

southern part of St. Helena Sound over this interval. The remaining deposition occurred at Fripp inlet (area 10) and and on the southern margin of the Hunting Island Platform (area 11).

During the 1914/20–1973 (53 years) interval, Hunting Island and the adjacent nearshore region experienced total erosion of 22.94 million m³ or an average net erosion rate of 433,000 m³/year (Fig. 6B and Table 1B). Much of this erosion (50%) occurred in St. Helena Sound (areas 2, 3, and 4). A major portion (30%) of the erosion occurred along the Hunting Island shoreline (area 1). However, unlike the previous interval, the inner platform region experienced no measurable erosion. The Hunting Island shoreline eroded at an average rate of 131,000 m³/year. The remaining erosion (20%) occurred at Fripp Inlet (areas 5, 6, and 7).

Total deposition during the interval 1914/20 to 1973 amounted to 24.25 million m³ or an average net deposition rate of 458,000 m³/year. About 51% of this deposition occurred on the outer margins of the Hunting Island Platform (areas 12 and 13). About 28% occurred in St. Helena Sound (areas 14, 15, and 16) and 21% at Fripp Inlet (areas 8, 9, 10, and 11).

During the entire 1856–1973 interval, total erosion amounted to 39.08 million m³ and total deposition amounted to 37.70 million m³. The amounts of erosion and deposition are almost equal (less than 4% difference).

Table 1A. *Erosion and deposition volumes for the interval 1856–1914/20. These areas are located in Figure 6A. Volumes are × 10³ m³. The Hunting Island Platform is that part of the St. Helena Sound ebb tidal delta adjacent to the southern part of the sound and Hunting Island.*

| Location | Erosion | | Deposition | |
|---|---|---|---|---|
| | Area | Volume | Area | Volume |
| Hunting Island Region | 1 | 7,280 ± 1,140 | | |
| | 2 | 2,430 ± 470 | | |
| | 3 | 1,530 ± 260 | | |
| | 4 | 380 ± 200 | | |
| St. Helena Sound (southern part) | 5 | 1,240 ± 530 | 12 | 660 ± 340 |
| | 6 | 1,050 ± 320 | 13 | 9,350 ± 1,560 |
| | 7 | 1,260 ± 470 | 14 | 1,060 ± 450 |
| | 8 | 390 ± 200 | 15 | 700 ± 260 |
| Fripp Inlet | 9 | 580 ± 340 | 10 | 930 ± 430 |
| Hunting Island Platform | | | 11 | 750 ± 270 |

Table 2. *Mean settling speed (χ) and sorting for beach transects along Harbor, Hunting, and Fripp Islands. Values are in CHI units. Five replicate samples were taken at every site along each transect.*

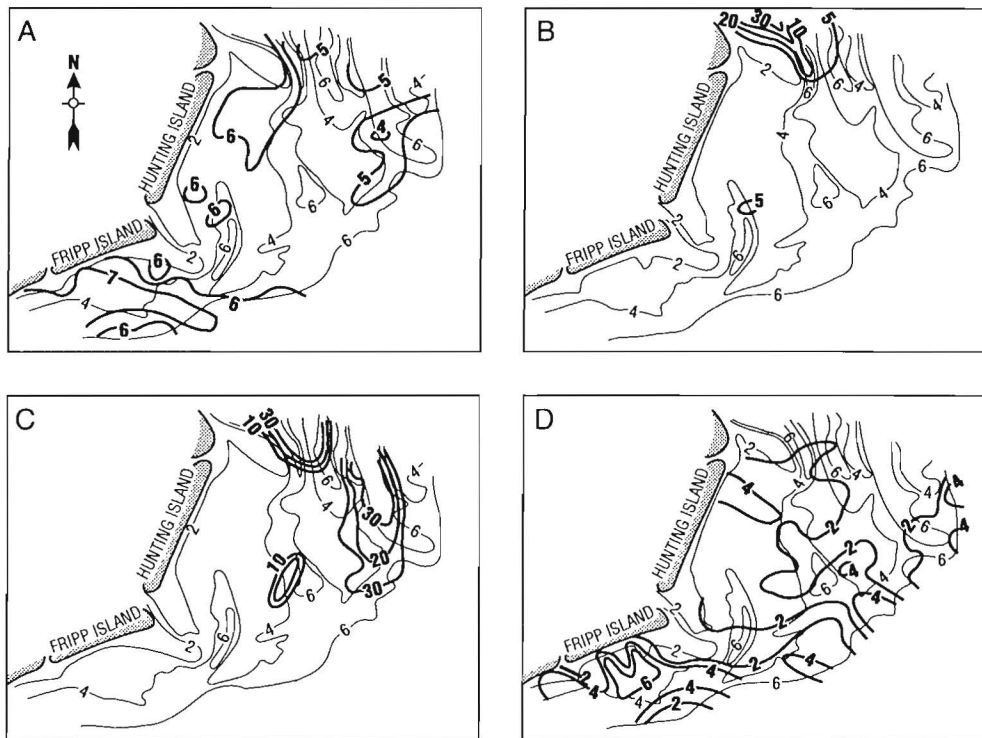| Transect Location | No. of Sites | Mean Speed | Sorting |
|---|---|---|---|
| HB-1 | 12 | 5.6 ± 0.1 | 0.40 ± 0.04 |
| HI-1 | 9 | 5.7 ± 0.1 | 0.53 ± 0.10 |
| HI-2 | 9 | 5.8 ± 0.1 | 0.54 ± 0.10 |
| HI-3 | 9 | 5.7 ± 0.1 | 0.54 ± 0.04 |
| HI-4 | 8 | 5.8 ± 0.1 | 0.47 ± 0.08 |
| HI-5 | 10 | 5.8 ± 0.1 | 0.51 ± 0.09 |
| FI-1 | 9 | 5.7 ± 0.2 | 0.48 ± 0.08 |
| FI-2 | 14 | 5.8 ± 0.1 | 0.48 ± 0.06 |

Figure 7. Characteristics of the surficial sands that cover the Hunting Island Platform: A. quartz mean-settling-speed ($\chi$ units, see text); B. weight percent silt/clay; C. weight percent calcium carbonate (shell); D. weight percent heavy minerals.

## Sand Analysis

### 1. Beach sands (Table 2):

Sample analyses for carbonate and heavy mineral content showed no significant trends. Silt/clay content was insignificant. Sand settling analysis indicated very homogeneous conditions along the beach. No trends in mean settling speed that might correlate with longshore drift direction were discernable.

### 2. Hunting Island Platform sands:

Most of the platform sands were characterized by relatively homogeneous quartz sand; however, based on settling tube analysis, some weak trends in grain-size distribution can be observed (Fig. 7A). The coarser sands (lower $\chi$ values) are associated with the tidal channels along the north margin of the platform and along the outer edges of the platform to the southeast and south. These sands have settling speeds that are generally in the range of 4–5 $\chi$ (6–3 cm/sec or 1–2 Phi). The remainder of the platform sands are in the range 5–6 $\chi$ (3.1–1.6 cm/sec or 2–3 Phi).

Silt/clay percentages are greatest along a tidal channel on the north edge of the platform (Fig. 7B). There appears to be a correlation of occurrence of silt and clay with higher $CaCO_3$ concentrations (Fig. 7C).

The highest carbonate concentrations are associated with the tidal channels along its northern margin (Fig. 7C). This

material consists primarily of shell debris that is typically of coarse size and is found on channel bottoms where tidal-current velocities are high.

Heavy minerals constitute from 2 to 4 percent by weight of the platform sands (Fig. 7D). There is a weak tendency for higher concentrations to correlate with the occurrence of finer-grained sands (Fig. 7A), as can be observed to the south off Fripp Island.

## Wave Current Analysis

The significant-wave simulation with the WAVENRG model and input based on the Oceanographic Atlas (USN) and wave-gage (CERC) data indicate that net longshore drift along Hunting Island is predominantly northward (Fig. 8). There is a predicted zone of erosion along the southern third of the island and a zone of deposition along the northern two-thirds. Based on field evidence, the boundary between erosion and deposition is actually farther north, with deposition occurring at the extreme northern end of the island only. Maximum net drift volumes are predicted to be on the order of only 8,000 $m^3$/year; however, gross drift is predicted to be about 80,000 $m^3$/year. The significant-wave height and period used in this analysis were 1 m and 6.5 sec. respectively (THOMPSON, 1977).

The significant-wave analysis does not adequately represent sand transport during storms. As wave energy increases as the square of the wave height, storm waves may move a
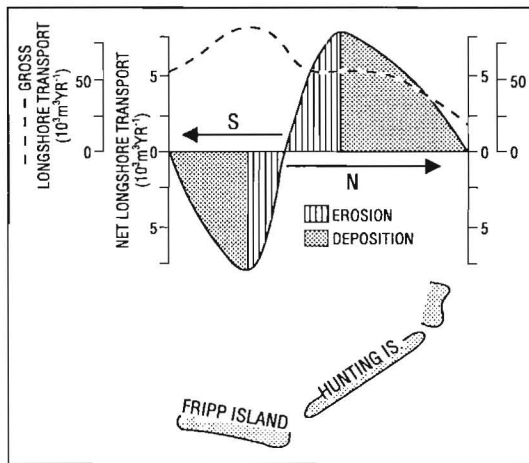
Figure 8. WAVENRG simulation of longshore drift at Hunting Island fair-weather, significant-wave conditions. Gross drift refers to the total volume of material that waves can entrain at the beach. Approach directions and frequencies were taken from Oceanographic Atlas (U. S. Navy, 1963) data. A significant, deep-water wave of 1 m height and 6.5 s period, obtained from CERC wave-gage data (Thompson, 1977) collected at the Savannah Light Station, was modeled in this computer simulation.

larger volume of sand than would be suggested simply by their frequency of occurrence. Storm conditions were simulated by using the 95th percentile (THOMPSON, 1977) wave height (3 m) and period (11.5 sec.). The simulation (Fig. 9) predicts a net longshore drift of about 2,500 m³/year to the north, with gross drift of about 25,000 m³/year. Adding significant or fair-weather to storm longshore drift yields a predicted net drift of about 10,500 m³/year to the north. Gross longshore drift is predicted to be about 105,000 m³/year.
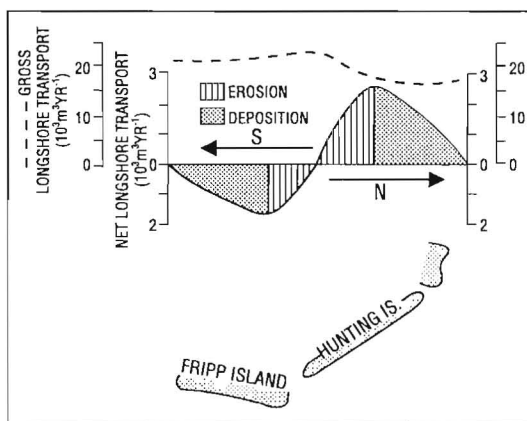


Figure 9. WAVENRG simulation of longshore drift at Hunting Island during storm conditions. The 95th percentile height (3 m) and period (11.5 sec) of CERC wave-gage data (Thompson, 1977) collected at the Savannah Light Station were used to estimate storm conditions. Approach directions used in this simulation were east-northeast, east, east-southeast, southeast, south-southeast, and south; frequencies, also based on the 95th percentile, were taken from the Oceanographic Atlas (U. S. Navy, 1963).
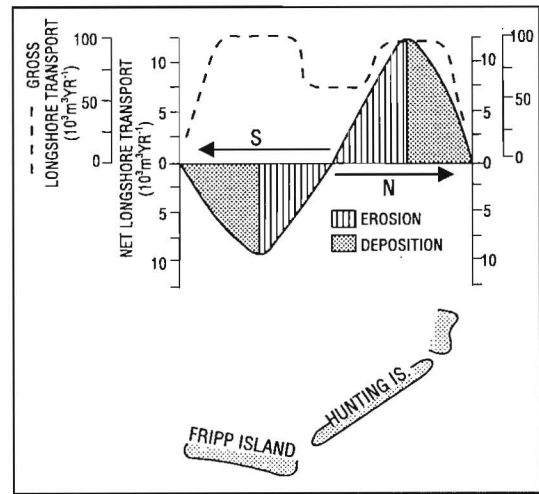


Figure 10. WAVENRG simulation of longshore drift at Hunting Island based on a wave climate determined by WIS meteorological hindcast (Corson et al., 1981).

The simulation based on meteorological hindcasts (Fig. 10) indicates similar results. As these data, unlike the USN data, provide directional frequencies of wave height and period, a separate "storm run" was not necessary. Net longshore drift was predicted to be northward at a rate of about 12,000 m³/year and gross drift at about 100,000 m³/year, values similar to those based on the USN data.

Wave-caused currents at the bottom induce a shear stress on the bottom sands. These were found (Fig. 11) to range from 1.0–4.0 dynes/cm² for a flat-bed model and from 3.4 to >9.0 dynes/cm² for the rippled bed model (STERNBERG, 1972), sufficient to entrain the sands present on the Hunting Island Platform.
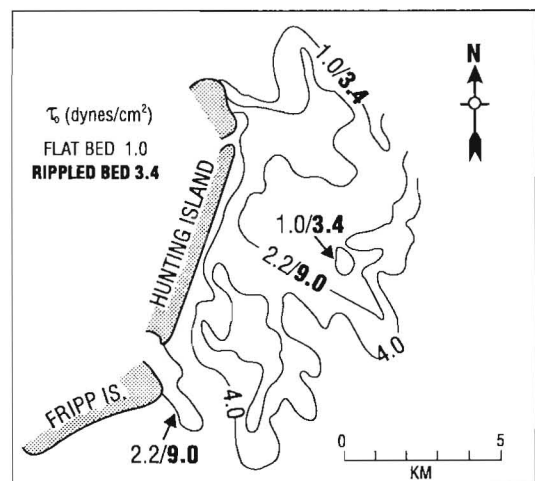


Figure 11. Distribution of bottom shear stresses due to waves based on velocity computations from the WAVENRG simulation program.
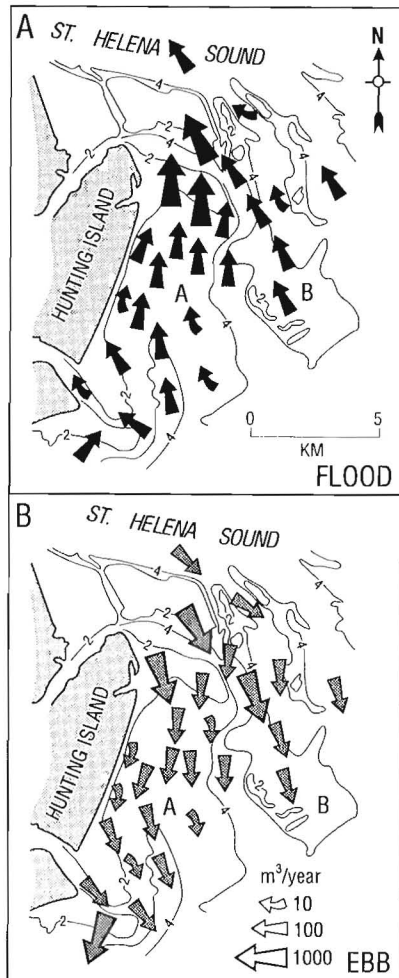
Figure 12.    A. Flood sand transport vectors (m³/m/year) for the Hunting Island Region. B. Ebb sand transport vectors for the Hunting Island Region. These vectors were calculated 1) for tidal channels using the Sternberg (1972) formula for instantaneous bedload transport and 2) for the wave- and tide-influenced Hunting Island Platform using the Sternberg (1972) formula with the Swart (1976) modification for wave/current interaction.



Figure 13.    Net sand-transport vectors, in m³/m/year, for the Hunting Island region Northward (flood) net transport dominates the inner Hunting Island Platform, including the area adjacent to the beach Southward (ebb) net transport dominates on the outer platform and in the tidal channels of southern St Helena Sound. Over the past 50 years almost all of the net deposition measured offshore is along the western margin of the outer Hunting Island Platform, site 13 of Figure 5B, the boundary between flood- and ebb-directed transport

## Tidal Current Analysis

Analysis of current meter data indicates that the narrow tidal-channels in the southern part of St. Helena Sound and the outer Hunting Island Platform are ebb-dominant with net flow directed to the southeast and south. The inner Hunting Island Platform is primarily flood-dominant with flow directed to the north. A narrow, ebb-dominant region occurs 2–3 kilometers offshore and extends the entire length of Hunting Island.

## Sand Transport System Analysis

Ebb and flood sand transport vectors for the Hunting Island Region were calculated 1) for tidal channels using the STERNBERG (1972) formula for instantaneous bedload trans-
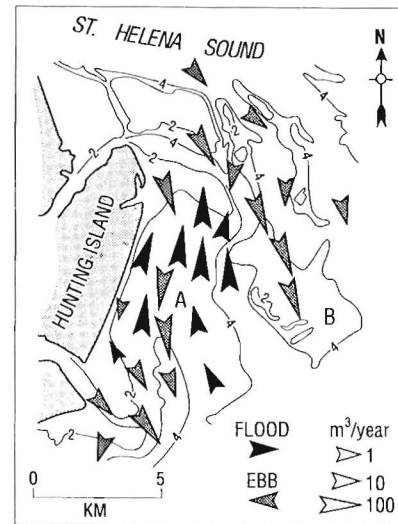
port and 2) for the wave- and tide-influenced Hunting Island Platform using the STERNBERG (1972) formula with the SWART (1976) modification for wave/current interaction. Ebb and flood sand transport vectors are illustrated separately (Fig. 12). Integrating these data into a single model, the following sand transport regions can be detected (Fig. 13):

1. A strip 1–2 km wide that lies adjacent to the Hunting Island shoreline that is characterized by net northward drift, indicating flood dominance;
2. A narrow strip just seaward of the coastal strip with southward drift, indicating ebb dominance;
3. A third parallel strip 2–3 km wide with northward drift indicating flood dominance;
4. A fourth, outer strip several km wide with southward drift that is a continuation of southeastward drift debouching from St. Helena Sound, indicating ebb dominance;
5. Drift vectors near Fripp Inlet indicate ebb dominance in the inlet and southwest drift towards Fripp Island immediately offshore from the inlet.

### DISCUSSION

#### Bathymetric Analysis

The geographic juxtaposition of major erosion and deposition sites, the geomorphologic setting at the mouth of a tidal estuary, and the "balance" between eroded and deposited volumes strongly suggest that material eroded from Hunting Island is transported north into St. Helena Sound and then out onto the adjacent ebb tidal delta. These sand budget data

describe two distinct conditions for Hunting Island and two for the southern part of St. Helena Sound.

During the 1856–1914/20 interval, erosion was concentrated primarily at the northern portion of the Hunting Island region, both along the beach and in the nearshore. This period was followed by erosion spread uniformly all along Hunting Island, but restricted to the beach and breaker zone in the 1914/20–1973 interval. During the earlier interval the southern part of St. Helena Sound served as a deposition site, the influx of material from Hunting Island resulting in the modification of tidal channels and shoals. In the 1914/20–1973 interval this part of the sound experienced net erosion. Material both introduced from Hunting Island and locally eroded from shoals was transported through tidal channels out onto the ebb tidal delta and deposited on the outer Hunting Island platform.

## Sand Analysis

Coarser particles indicate higher energy levels and should occur where tidal and wave currents are greatest. Their occurrence in the ebb tidal channels is to be expected given the high current velocities that occur there. Their occurrence on the outer edge of the platform results from two effects. First, this is where the relatively coarser sands debouch from the mouths of the ebb tidal channels. Secondly, this is the location of a zone of a relatively higher wave-energy level there than farther inshore. This situation is due to the shallowness of the platform. Deep water waves progressing shoreward from the Atlantic Ocean strike the edge of the platform and lose much of their energy through bottom friction as they proceed across it. The bottom currents produced by the waves are greater along the outer edge of the platform, diminish across the central region of the platform, and increase again at the surf zone.

## Wave Analysis

The salient points brought out by this computer simulation of longshore drift are: (1) net longshore drift along the Hunting Island beach is an order of magnitude less than the measured rate of shoreline erosion based on map differencing and beach renourishment and (2) the amount of material entrained along the beach by wave action, the gross drift, is reasonably close to these measured erosion rates.

Wave-orbital velocities at the bottom estimated by the WAVENRG program using deepwater wave parameters indicate that significant waves will entrain sand across almost all of the width of the Hunting Island Platform (Fig. 11) and should transport it landward. Little, if any, of this material ever reaches the beach.

## Tidal Current Analysis

Tidal circulation controls sand transport on the Hunting Island Platform (Fig. 13). Ebb-directed currents dominate the tidal channels of southern St. Helena Sound as well as the outer Hunting Island Platform. Flood-directed currents dominate the inner part of the platform immediately offshore of the Hunting Island beach and all along the inner margin of

the outer Hunting Island platform. A 1–2 km-wide belt of ebb-directed currents extending along the entire length of the inner platform divides these two regions of flood-directed movement.

## A Sand Transport Model for Hunting Island

Sand transport modeling at Hunting Island indicates the presence of an integrated system that results from the combined effects of waves and tidal currents acting across the broad, shallow Hunting Island Platform in concert with the tidal channels exiting St. Helena Sound to the north.

Sand transport along the Hunting Island beach is significantly affected by the Hunting Island Platform. The platform serves to shelter Hunting Island from waves, the effectiveness of which is readily apparent considering the rather low net littoral transport rate of 11,000 m³/year predicted by the WAVENRG computer simulation. However, this simulation also predicts that waves at the shoreline produce a gross (bidirectional) drift of 100,000 m³/year. For at least the past half century the outer Hunting Island platform has been attached by an intertidal shoal extending virtually intact from the northern tip of Hunting Island. The deeper, ebb-dominant, tidal channels of St. Helena Sound do not exit immediately in front of Hunting Island, but rather empty into the outer platform several kilometers offshore. This bathymetric configuration causes the funnel-shaped inner portion of the platform to be flood-dominant. Hunting Island beach erosion is then hypothesized to be a two-step process with *entrainment* accomplished by waves operating nearly uniformly all along the shore and *transport* performed by the combined effect of longshore currents and flooding tidal currents moving northward into St. Helena Sound. A minor component is directed southward into Fripp Inlet. The Hunting Island erosion rate as determined from map differencing and beach nourishment of 130,000 m³/year agrees remarkably well with the combined littoral and gross drift of 100,000 m³/year predicted by the WAVENRG computer simulation.

The fate of material eroded from the Hunting Island beach can be inferred from a combination of map differencing and bottom tidal-current data. Over the period 1914/20–1973 a major deposition site developed on the western margin of the outer Hunting Island Platform (site 13 in Fig. 6B and Table 1B). Erosion along the southern margin of St. Helena Sound can account for approximately 45% of the material deposited at this site. The bottom tidal current data indicate that northward currents dominate the nearshore region, the inner platform. A significant proportion of the material eroded from the beach must move north into St. Helena Sound and a minimum estimate of this amount is the 100,000 m³/year needed to complete the amount deposited in site 13. The remainder of the eroded material, on the order of 25,000 m³/year, may move southward into Fripp Inlet where it would make a minor contribution to the measured budget (Fig. 6B and Table 1B).

Deposition site 13 on the western margin of the outer Hunting Island platform is located along the boundary between tidal flow into and out of St. Helena Sound. In addition, flood-dominant tidal currents sweeping through the fun-
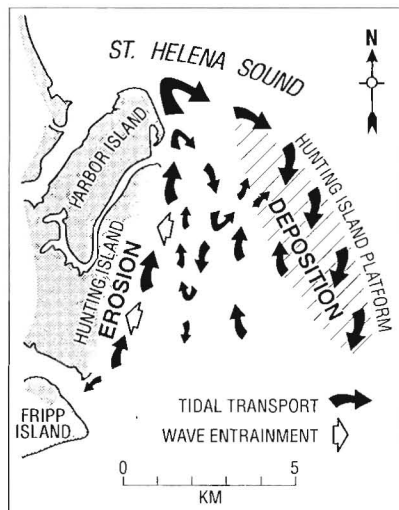
Figure 14. Summary diagram illustrating the hypothesized sand transport in the Hunting Island region. Beach erosion along Hunting Island is a two-step process with 1) entrainment accomplished by breaking waves and 2) transport performed by flooding tidal-currents. Sand removed from Hunting Island is moved northward into southern St. Helena Sound and then seaward through ebb-dominant tidal channels to be deposited on the western margin of the outer Hunting Island Platform. The flood-dominant character of the inner platform inhibits the landward movement of sand from the outer platform that would otherwise replenish the eroding beach.

nel-shaped inner platform inhibit the landward transport of sand due to shoaling waves by shunting material northward into St. Helena Sound. The Hunting Island beach is effectively isolated from its natural source of replenishing sand (Fig. 14).

## CONCLUSIONS

Based on the sand characteristics and wave/tide currents, a model was formulated to describe the sand transport system that exists in the Hunting Island region. The model was compared to the historical changes revealed by map differencing that have taken place over the past century in an effort to evaluate its validity in accounting for those changes, as well as serving as a predictive tool.

Beach erosion at Hunting Island is a two step process with entrainment accomplished by waves and transport performed by combined longshore and tidal currents flooding northward. Sand removed from this beach is moved northward into St. Helena Sound and then through ebb-dominant tidal channels out onto the adjacent portion of the ebb tidal delta, the outer Hunting Island Platform. The funnel-shaped inner platform separating Hunting Island from the outer platform is flood-dominant, which causes sand that might be transported shoreward by shoaling waves to be delivered northward into St. Helena Sound and then back to the outer platform. Hence, the Hunting Island beach is effectively isolated from the potential source of replenishing sand that is located offshore.

## LITERATURE CITED

ANDERS, F. J., REED, D. W., AND MEISBURGER, E. P., 1990. Shoreline Movements; Report 2, Tybee Island, Georgia, to Cape Fear, North Carolina, 1851–1983. Technical Report CERC-83-1, US Army Engineer Waterways Experiment Station, Vicksburg, MS, 152 p.

BAGNOLD, R. A., 1946. Motions of waves in shallow water; interaction between waves and sand bottoms: Proceedings Royal Soc. London, 187, series A, 1–15.

BAGNOLD, R. A., 1963. Mechanics of marine sedimentation. in HILL, M. N. (ed.), The Sea, Vol. 3: The Earth Beneath the Sea, Wiley—Interscience, New York, 507–528.

CARTER, R. W. G., JENNINGS, S. C., and ORFORD, J. D., 1990. Headland erosion by waves. Journal of Coastal Research, 6(3), 517–529.

CSE, 1990. Erosion assessment and beach restoration alternatives for Hunting Island, South Carolina. Feasibility Study for South Carolina Dept. of Parks, Recreation, and Tourism. Coastal Science and Engineering, Inc., unpublished report dated July 1990, 66p.

CSE, 1991. Hunting Island State Park 1991 Beach Nourishment Project, Survey Report No. 1, unpublished report dated August 1991.

CORSON, W. D., RESIO, D. T.; BROOKS, R. M.; EBERSOLE, B. A.; JENSEN, R. E.; RAGSDALE, D. S., and TRACEY, B. A. 1981. Atlantic coast hindcast, deepwater, significant wave information: WIS Report No. 2, U. S. Army Engineer Waterways Experiment Station, Vicksburg, Miss., 17 p., 14 Appendices.

CORSON, W. D., RESIO, D. T., BROOKS, R. M.; EBERSOLE, B. A., JENSEN, R. E.; RAGSDALE, D. S., and TRACEY, B. A. 1982. Atlantic Coast Hindcast, Phase II Wave Information: WIS report No. 6, U. S. Army Engineer Waterways Experiment Station, Vicksburg, Miss., 1186 p.

GRANT, W. D., and MADSEN, O. S., 1979. Combined wave and current interaction with a rough bottom. Journal of Geophysical Research, 84, 1797–1808.

GREENWOOD, B., and McGILLIVRAY, D. G., 1978. Theoretical model of the littoral drift system in the Toronto waterfront area, Lake Ontario. Journal Great Lakes Research, 4, 84–102.

HAMMOND, T. M., and COLLINS, M. B., 1979. On the threshold of transport of sand-sized sediment under the combined influence of unidirectional and oscillatory flow: Sedimentology, 26, 795-812.

HUBBARD, D. K.; BARWIS, J. H., LESESNE, F., STEPHEN, M. F. and HAYES, M. O., 1977. Beach erosion inventory of Horry, George town, and Beaufort Counties, South Carolina: Technical Report No. 8, South Carolina Sea Grant, 58 p.

JENSEN, R. E., 1986. Atlantic Coast Hindcast, Shallow-water Significant Wave Information: WIS Report No. 9, U. S. Army Engineer Waterways Experiment Station, Vicksburg, Miss., 711 p.

JONSSON, I. G., 1966. Wave boundary layers and friction factors. Proceedings, 10th Conf. Coastal Engineering, 127–148.

KOMAR, P. D. and INMAN, D. L., 1970. Longshore sand transport on beaches. Journal of Geophysical Research, 75, 5914–5927.

KOMAR, P. D. and MILLER, M. C., 1973. The threshold of sediment movement under oscillatory waves: Journal Sedimentary Petrology, 43, 1101–1110.

KOMAR, P. D. and MILLER, M. C., 1975. On the comparison between the threshold of sediment motion under waves and unidirectional

currents with a discussion of the practical evaluation of the threshold: Journal Sedimentary Petrology, 45, 362–367.

KOMAR, P. D., 1976. Beach Processes and Sedimentation. Prentice-Hall. Inc., Englewoods Cliffs, N. J., 429 p.

LARSEN, L. H., STERNBERG, R. W., SHI, N. C., MARSDEN, M. A. H., and THOMAS, L., 1981. Field investigations of the threshold of grain motion by ocean waves and currents. Marine Geology, 42, 105–132.

LOWRY, P., and CARTER, R. W. G., 1982. Computer simulation and delimitation of littoral power cells on the barrier coast of Southern County, Wexford, Ireland. Journal of Earth Science, Royal Dublin Soc., 4, 121–132.

MADSEN, O. S., and GRANT, W. D., 1975. The threshold of sediment motion under oscillatory waves: a discussion: Journal Sedimentary Petrology, 45, 360–361.

MADSEN, O. S. and GRANT, W. D., 1976. Sediment transport in the coastal environment: Ralph M. Parsons Lab for Water Resources and Hydrodynamics, Rept. 209, Department of Civil Engineering, Mass. Institute of Technology, Cambridge. 105 p.

MANOHAR, MADHAV, 1955. Mechanics of bottom sediment movement due to wave action: U. S. Army Corps of Engineers, Beach Erosion Board, Tech. Memo No. 75, 121 p.

MATHEWS, T. D.; STAPOR, F. W.; RICHTER, C. R.; et al. (Eds.), 1980. Ecological characterization of the Sea Island coastal region of South Carolina and Georgia. Vol. 1: Physical features of the characterization area: U. S. Fish and Wildlife Service, Office of Biological Services, Washington D. C., Fws/obs-79/40, 212 p.

MAY, J. P. and TANNER, W. F., 1973. The littoral power gradient and shoreline changes: in Coastal Geomorphology, D. R. COATES (Ed.), Publications in Geomorphology, State University of New York, Binghampton, 43–60.

MAY, J. P., 1973. Sedimentary and geomorphic response to systematic variation of wave energy in the nearshore zone: unpublished Ph.D. dissertation, Dept. of Geology, Florida State University, Tallahassee, Florida, 209 p.

MAY, J. P., 1974. WAVENRG: a computer program to estimate the distribution of energy dissipation in shoaling waves with examples from coastal Florida: in Nearshore Sediment Transport, W. F. TANNER (Ed.), Dept. of Geology, Florida State University, Tallahassee, Florida, 22–80.

MAY, J. P., 1977. Ability of various water wave theories to predict maximum bottom orbital velocities in the shoaling wave zone. Coastal Research Notes, 4, 7–9.

MAY, J. P., 1981. CHI (X): a proposed standard parameter for settling tube analysis of sediments: Journal Sedimentary Petrology, 51, 607–610.

MILLER, M. C., McCAVE, I. N. and KOMAR, P. D., 1977. Threshold of sediment motion under unidirectional currents: Sedimentology, 24. 507–527.

NUMMEDAL, D., OERTEL, G. F., HUBBARD, D. K. and HINE, A. C., 1977. Tidal inlet variability—Cape Hatteras to Cape Canaveral:

Coastal Sediments '77, American Society of Civil Engineers, 345 East 47th Street, New York, NY, 10017, 543–562.

PATTIARATCHI, C. B. and COLLINS, M. B., 1985. Sand transport under the combined influence of waves and tidal currents: an assessment of available formulae. Marine Geology, 67, 83–100.

PIERCE, J. W., 1969. Sediment budgets along a barrier island chain: Sedimentary Geology, 3, 5–16.

ROUSE, H, 1938. Fluid Mechanics for Hydraulic Engineers. Dover Publications Inc., New York, 422 p.

SALLENGER, A. H.; GOLDSMITH, V. and SUTTON, C. H., 1975. Bathymetric comparisons: a manual of methodology, error criteria and techniques: Special Report No. 66 in Applied Marine Science and Ocean Engineering, Virginia Institute of Marine Science, Gloucester Point, Virginia, 23062, 34 p.

SHIELDS, A., 1936. Anwendung der Ahnlichkeits Mechanik und der Turbulenzforschung auf die Geschiebe Bewegung: Preuss. Versuchanstalt fur Wasserbau und Schiffbau, Berlin, 20 p.

STAPOR, F. W., 1971. Sediment budgets on a compartmented low-to-moderate energy coast in northwest Florida: Marine Geology, 10 (2), M1-M7.

STAPOR, F. W. and MATHEWS, T. D., 1983. Higher-than-present Holocene sea-level events recorded in wave-cut terraces and scarps: Old Island, Beaufort County, South Carolina: Marine Geology, 52 (3/4), M53-M60.

STAPOR, F. W., and MAY, J. P., 1981. Sediment transport at Hunting Island, South Carolina. in Hunting Island State Park Beach Erosion Study, unpublished report prepared for S. C. Department of Parks, Recreation, and Tourism, dated July, 1982.

STEPHEN, M. F., BROWN, P. J., FITZGERALD, D. M., HUBBARD, D. K. and HAYES, M. O., 1975. Beach erosion inventory of Charleston County, South Carolina: a preliminary report: Technical Report No. 4, South Carolina Sea Grant, 79 p.

STERNBERG, R. W., 1972. Predicting initial motion and bedload transport of sediment particles in the shallow marine environment: in Shelf Sediment Transport: Processes and Patterns (SWIFT, D. J. P., DUANE, D. B., and PILKEY, O. H., Eds.), Dowden, Hutchinson, and Ross, Stroudsburg, PA, 61–82.

STONE, G. W., STAPOR, F. W., JR., MAY, J. P., and MORGAN, J. P., 1992. Multiple sediment sources and a cellular, non-integrated, longshore drift system: Northwest Florida and Southeast Alabama coast. USA. Marine Geology, 105, 141–154.

SUNDBORG, A., 1956. The River Klaralven: A Study of Fluvial Processes: Geografiska Annaler, 38, 127–316.

SWART, D. H., 1976. Coastal sediment transport: computation of longshore transport. Report R 968, Waterloopkundig Laboratorium (Delft Hydraulics Laboratory), 61 p.

THOMPSON, E. F., 1977. Wave climate at selected locations along U.S. coasts. Technical Report No. 77-1, U. S. Army Corps of Engineers, Coastal Engineering Center, 364 p.

U. S. NAVY, 1963. Oceanographic Atlas of the North Atlantic Ocean: Section IV Sea and Swell: U. S. Naval Oceanographic Office, Publication No. 700.